Vol. **99** (1901) *ACTA PHYSICA POLONICA A* No. 1

Proceedings of the International Workshop NOA'00, Grybów 2000

POLARIMETRIC FIBER-OPTIC SYSTEM FOR STATIC AND DYNAMIC STRAIN MEASUREMENT

W. Konopka*, T.R. Woliński, A.W. Domański and M.A. Karpierz

Faculty of Physics, Warsaw University of Technology
Koszykowa 75, 00-662 Warszawa, Poland

Polarization properties of the transmitted optical signal in polarimetric fiber-optic sensing systems for dynamic strain measurements as well as for smart structures applications are presented. The smart structure consists of highly birefringent fiber embedded in an epoxy cylinder.

PACS numbers: 42.81.Gs, 42.81.Pa

1. Introduction

Fiber-optic sensing systems are being presently tested in a variety of smart structures and skins applications [1–4]. In particular, polarimetric sensors with highly birefringent (HB) polarization-maintaining optical fibers have focused a great interest for use in conjunction with composite materials. This growing interest has been mainly manifested in successful applications of HB fibers into fiber optic sensors based on polarimetric interference [4]. An influence of a variety of physical parameters on the mode propagation in HB fibers is of special importance, since a number of physical quantities can be measured on the basis of the fibers. Recently, the suitability of HB few-mode fibers for the measurement of hydrostatic pressure, twist, and static and dynamic strain has been successfully demonstrated [4–9].

There is at present much effort to apply polarimetric fiber-optic sensors to measure strain in aircraft or concrete structures using a concept of so-called smart skins and structures. Smart structures or smart skin are structural components with networks of fiber optic sensors embedded in the composite material matrices. The composite materials are made from epoxies or polyimides. A more ambitious and complex use of smart structures involves linking fiber optic sensors with the real-time computer-control systems. In this model, fiber-optic sensors are embedded in a panel to be integrated with the plane wing or the construction. The sensors monitor environmental effects such as strain and bending. In response to

*corresponding author; e-mail: konopka@if.pw.edu.pl

computer output, a fiber optic link could drive remote actuators. Thus, a complete smart structure would not only detect problems but also respond to them instantaneously.

Fiber optic sensing systems can also be applied to perform a dynamic strain measurement. Such a system can be applied in the railway industry for wheel flatness checking.

The paper presents results of studies on the optical response of highly-birefringent-fibers based sensors and structures. Two different experimental configurations were considered where hydrostatic pressure and dynamic strain were applied.

2. Theoretical background

Highly birefringent polarization-maintaining fibers have a built-in, well-defined high internal birefringence. HB fibers are obtained by designing a core with non-circular (mostly elliptical) geometry or by introducing asymmetric stress over the core of the fiber, either by means of elliptical cladding or by fabricating the fiber with two regions of highly doped glass located on opposite sides of the core. Birefringence can also be created whenever a fiber undergoes elastic stresses resulting from external perturbations such as hydrostatic pressure, longitudinal strain, squeezing, twisting, and bending, etc. The external perturbation through the photoelastic effect lifts the degeneracy of the linearly polarized modes and induces extrinsic birefringence. Thus, the modal behavior of the lowest-order mode HB fibers under various external deformations is of special interest for sensors and devices. A number of physical quantities can be measured on the basis of two-mode HB fibers: hydrostatic pressure, strain, vibration, temperature, acoustic wave, etc.

A symmetric deformation effect influences the propagation constant β_i in every mode. It occurs due to changes of optical fiber length (L) and the refractive indices of the core and the cladding. This leads to changes in the phase $\Phi_i = \Delta\beta_i L$ along the fiber

$$\delta\Phi_i = \delta(\Delta\beta_i)L + \Delta\beta_i \delta L, \tag{2.1}$$

where $i = x,\ y$; $\delta\Phi_x$ and $\delta\Phi_y$ are the phase changes of two orthogonal polarization modes LP_{01}^x and LP_{01}^y.

If the external perturbation is denoted by ξ, then an increase by $\delta\xi$ will cause a change in both, the $\Delta\beta_i$ and the L by $\partial(\Delta\beta_i)/\partial\xi$ and $\partial L/\partial\xi$. Thus, from (2.1) it is obtained that

$$\delta\Phi_i = \left[\frac{\partial(\Delta\beta_i)}{\partial\xi}L + \Delta\beta_i\frac{\partial L}{\partial\xi}\right]\delta\xi = \frac{2\pi}{T_{i,\xi}}\delta\xi = \Lambda_{i,\xi}\delta\xi. \tag{2.2}$$

The quantities $T_{i,\chi} (i = x,\ y$ and $\chi = \xi)$ have the dimension of the measurand ξ while $\Lambda_{i,\chi}$ have the inverse dimension. These are experimentally measurable parameters that determine the sensitivity of the sensor to a given external perturbation.

$\delta\Phi_x$ and $\delta\Phi_y$ are responsible for the changes of the output polarization state of the light propagating in the fiber under deformation. In such a case the intermodal polarization interference between polarization modes LP_{01}^x and LP_{01}^y occurs and requires the use of an analyzer placed at the output of the fiber, see Fig. 1.

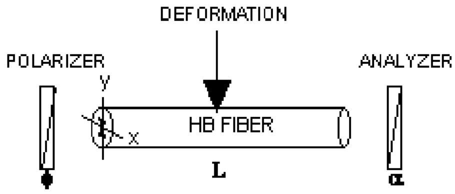

Fig. 1. Deformation effect in a HB fiber modulates light intensity after the analyzer.

Thus a deformation effect in a HB fiber modulates light intensity after the analyzer in the following manner:

$$I(z=L)=\frac{1}{2}(1+\cos 2\alpha\cos 2\phi+|\gamma_i|\sin\alpha\sin 2\phi\cos\Delta\Phi_i), \tag{2.3}$$

where $\Delta\Phi_i$ signifies the differential phase of the light exiting the HB fiber and γ_i is a mutual correlation function, ϕ is the angle between polarizer axis and birefringence axis, while α is the angle between analyzer axis and birefringence axis.

3. Experimental

The experimental set-up for optical response to hydrostatic pressure that included a pig-tailed laser diode at 633 nm wavelength, fiber optic transducer, detection system, and pressure chamber is presented in Fig. 2.

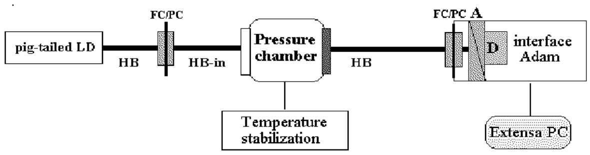

Fig. 2. Experimental set-up. Fiber optic transducer is connected to the EXTENSA-510 PC by the interface ADAM-4017; FC/PC — optical connectors, D — detector.

The pressure transducer was connected to the pig-tailed diode and detection system with FC/PC connectors. This makes the system more flexible and allows an easy rearrangement. An IBM-PC with a specially designed interface built on the base of advanced ADAM modules (Advantech Co., Ltd.) is used for data visualization. Pressure generation and calibration up to 300 MPa were performed by DWT pressure device. The proposed system is a step towards a commercial application of the smart structures based on polarization interferometry in fibers.

The lead-in and lead-out fibers are *fibercore bow-tie* highly birefringent waveguides. Sensing samples composed of *bow-tie* and *side-hole* birefringent fibers embedded in an epoxy structure (of the diameter 7 mm, and length 110 mm, Fig. 3), were investigated. To create the structures the EPIDIAN-5 epoxy glue (Young Modulus $E = 1273.13$ [N/mm^2]) was used.

The prepared polarimetric smart structures were subjected to deformation effects such as those induced by hydrostatic pressure and temperature, whereas polarization properties of the transmitted optical signal have been investigated.

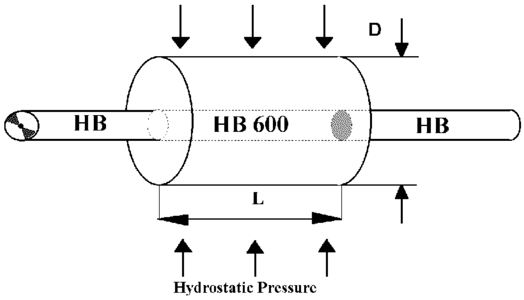

Fig. 3. Hi-Bi fiber embedded in the cylindrical epoxy structure.

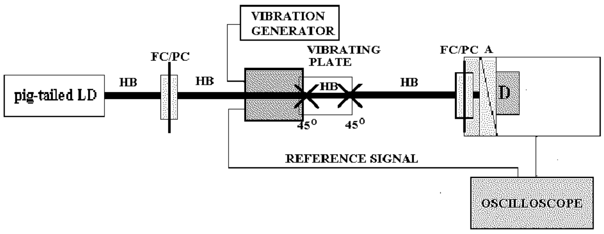

Fig. 4. Experimental set-up for measurement of the dynamic strain, D — detector, $\times_{45^\circ}$ — points where the fibers are spliced and the angle between birefringence axes.

The experimental set-up for optical response to dynamic strain that included a pig-tailed laser diode at 633 nm wavelength, fiber optic transducer, detection system, and vibrating plate is presented in Fig. 4. The transducer is glued on the vibrating piezoceramic plate. The plate is in fact composed of two plates, glued together — the one generating vibrations (connected with the vibration generator) and the other, connected to the oscilloscope, monitoring vibrations. The output optical signal is collected at the detector after passing through the analyzer, which is set along one of the fiber axis. Such a set-up enabled us to calibrate the dynamic sensor.

4. Results

The optical response of the different polarimetric fiber optic sensors under various external factors always shows sinusoidal behavior [4, 7–9], see Fig. 5a, b. However, for the sensor embedded in the structure one can observe a change of the period of sinusoidal characteristic. The *bow-tie* smart structure characteristic under hydrostatic stress has a fundamental period $T_\mathrm{p} \sim 100$ MPa, which is twice as much as the period of the characteristic of the same sensor without the epoxy structure, which is $T_\mathrm{p} \sim 50$ MPa. Both characteristics are presented in Fig. 5a. This means that the epoxy cylinder isolates (to some extent) the birefringent fiber from the external load.

Moreover it can be easily noticed (Fig. 5a,b) that the smart structure composed of *side-hole* fiber shows a much better sensitivity than the HB-600 *bow-tie*. Thus different HB fibers are suitable for different pressure ranges.

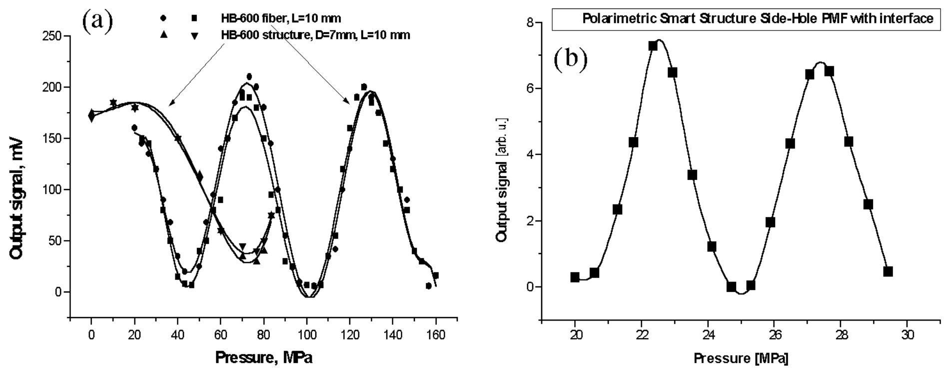

Fig. 5. (a) Comparison of the output characteristics of the separated *bow-tie* fiber sensor (up & down characteristics) and smart structure sensor based on the same sensing fiber (up & down characteristics). (b) Optical response of the smart structure based on *side-hole* (type V) birefringent fiber to the applied hydrostatic pressure.

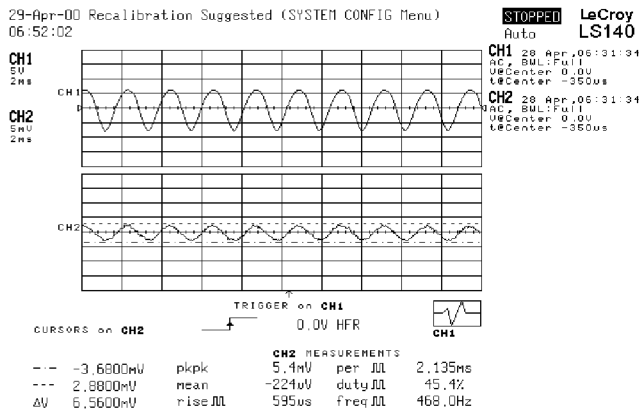

Fig. 6. Time dependence of the output signals of the monitoring plate (CH1) and the fiber optic sensor (CH2) recorded on the oscilloscope.

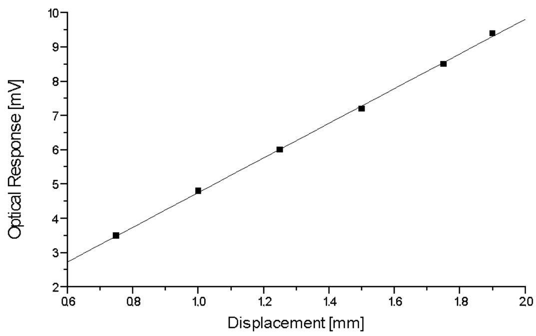

Fig. 7. Calibration curve of the fiber optic polarimetric sensor for the dynamic measurements.

The results of the dynamic strain measurements are presented in Fig. 6 that shows the output from the oscilloscope. The upper characteristic (CH1) is the reference signal generated by the monitoring plate, while the lower one (CH2) is the optical output signal. The producer of the device for vibration generation and monitoring has supplied us with the calibration curve for the plate that monitored the vibration. This enabled us to determine the displacement in [mm] introduced by the vibrating plate and create our own calibration curve of the fiber optic sensor for dynamic strain measurements, presented in Fig. 7.

5. Conclusions

The result of performed experiments shows that fiber optic polarimetric sensors are suitable for measurements of both static and dynamic external loads. Calibration of the dynamic sensor was performed with the device exploiting vibrating piezoceramic plate. The *bow-tie* fiber embedded in an epoxy container is suitable for a high pressure sensing application, whereas the *side-hole* smart structure is more suitable for smaller ranges but with a higher accuracy. We can also conclude that the epoxy structure isolates the fiber from the external load, but does not change the shape of optical response of the fiber optic polarimetric sensors.

Acknowledgments

The work was partially supported by the Photonics Engineering Research Project of the Warsaw University of Technology and by the Committee for Scientific Research (KBN) under the grant No. 8T11D01218. The authors are grateful to Dr. J. Wójcik (UMCS Lublin) for fruitful collaboration. The support of Ericsson Company is also gratefully acknowledged.

References

[1] E. Udd, *Fiber Optic Sensors*, J. Willey & Sons, New York 1991.

[2] T.R. Woliński, A.W. Domański, P. Gałązka, *Polarimetry and Ellipsometry,* Eds. M. Pluta, T.R. Woliński, *Proc. SPIE* **3094,** 218 (1997).

[3] J. Calero, Sou-Pan Wu, C. Pope, Shun Lien Chuang, J.P. Murtha, *J. Lightwave Technol.* **12,** 1081 (1994).

[4] T.R. Woliński, in: *Progress in Optics*, Ed. E. Wolf, Vol. XL, Elsevier Science B.V., North-Holland, Amsterdam 2000, p. 1.

[5] W.J. Bock, A.W. Domański, T.R. Woliński, *Appl. Opt.* **29,** 3484 (1990).

[6] W.J. Bock, T.R. Woliński, T. Eftimov, *Pure Appl. Opt., J. Eur. Opt. Soc.* **5,** 125 (1996).

[7] T.R. Woliński, W. Konopka, A.W. Domański, in: *Laser Interferometry IX: Techniques and Analyses,* Eds. M. Kujawińska, G.M. Brown, M. Takeda, *Proc. SPIE* **3478,** 421 (1998).

[8] W. Konopka, T.R. Woliński, A.W. Domański, in: *Interferometry'99,* Ed. M. Kujawińska, *Proc. SPIE* **3745,** 319 (1999).

[9] T.R. Woliński, W. Konopka, A.W. Domański, in: *Polarisation and Colour Techniques in Industrial Inspection,* Ed. E. Trutco, *Proc. SPIE* **3826,** 264 (1999).